Memoirs of the College of Science, University of Kyoto, Series A,
Vol. XXXI, No. 2, Article 11, 1967.

COLLISIONAL EMISSION SPECTRA AND IONIZED GASES IN NUCLEI OF GALAXIES

BY

Sumiko ITOH and Tomokazu KOGURE

Department of Astronomy, University of Kyoto

(Received November 9, 1966)

ABSTRACT

Collisional emission spectra of ionized gases are calculated as a function of electron temperature T_e and electron density N_e in the ranges $T_e=1\sim10\times10^4$°K and $N_e=10\sim10^6$/cm^3. The emission lines adopted here are the Balmer lines (H_α, H_β, H_γ) and the nebular lines of [OI], [OII], [OIII], [SII], [NII], [NeIII], and [NeV]. It is found that (1) when the collisional excitation and ionization from the second energy level are taken into consideration, the Balmer decrement becomes quite steep, particularly for $T_e\lesssim20{,}000$°K, and (2) the relative intensities show appreciable density dependence when $N_e\gtrsim10^4$.

Then the gross feature of collision spectra is compared with the observed spectra of nuclei of galaxies, for which the available data are compiled in the Appendix. The comparison shows that the variety in the observed spectra may be well within the variety of the predicted spectra. This also shows that (a) the excitation mechanism in the nuclei of galaxies is of collisional character, and (b) the physical state of the ionized gas can be varied one by one in wide ranges of both N_e and T_e.

1. Introduction

It has long been evident that the nuclei of galaxies often disclose the existence of ionized gases as indicated by [OII]λ3727 and other spectral lines. In the earlier surveys of emission lines, made by MAYALL (1939), HUMASON (1947) and summarized by BAADE-MAYALL (1951), the difference of spectral feature between the nuclear regions and the outer emission patches in galaxies has not been fully mentioned. In the catalogue of HUMASON-MAYALL-SANDAGE (1956), the description has been mainly given on the distribution of ionized gases in galaxies such as very nuclei, central bars, outer arms, emission patches, and so on. A general conclusion from these data was that ionized gases could usually be found throughout most of the late S and I_{rr} galaxies (up to 80%), particularly in the spiral arms and brighter emission patches, whereas the emission in E, SO, and Sa galaxies was usually observed with a lower fraction (less than 20%) only in their nuclear regions. This variance has been attributed to a higher concentration of ionized gases toward the center in early type than in later type galaxies.

Thereafter BURBIDGE-BURBIDGE (1962) and BURBIDGE (1962) have recognized, in S and I_{rr} galaxies, some remarkable difference in the emission spectra between

nuclear regions and outer emission regions, especially in the intensity ratio $H_\alpha/[NII]\lambda6583$. According to them, the ratio generally takes a value near 3.0 in outer regions while a value of unity or less in the nuclei of galaxies. This may be compared with the intensity ratio in the galactic nebulosity measured by JOHNSON (1950), who gives the mean value of 3.2 for 49 nebulae among which only four indicate the ratio lower than 2.0. It is then almost certain that the ionized gases in the outer emission regions are of the same nature as those of galactic nebulosity. For E and SO galaxies some evidence has been presented by MINKOVSKY-OSTERBROCK (1959) and OSTERBROCK (1960, 1962), who also emphasized the difference between the gas in the nuclei and that in a typical gas cloud in our Galaxy. BURBIDGE-BURBIDGE (1965) have affirmed the similar character of gases in the early type galaxies.

It is, however, to be mentioned that, even when we speak of the emission spectra in the nuclear regions of galaxies, there appears a large variety in their spectral feature. This is shown in Tables A1 and A2 in the Appendix, which are compiled from the observed data available at present.

The excitation mechanism and the physical state of ionized gases in the nuclei have so far been considered theoretically by several authors, principally from the two points of view, i. e., one is the radiative excitation by hot stars or by nonthermal radiation and the other is the collisional excitation in turbulent hot media or by corpuscular radiation from stars. There are also two ways of approach to find the actual processes in the nuclei. The first is the energetic consideration. For example, OSTERBROCK (1960) has shown that the energy could be sufficiently supplied by both mechanisms radiative as well as collisional so long as suitable processes are provided. The second is the spectral feature, for which theoretical consideration has been made through the works of MINKOWSKY (1955), MIYAMOTO (1956), PARKER (1964), and OSTERBROCK-PARKER (1965). Generally speaking, Balmer decrement is steeper in collisional than in radiative excitation, and, the strength of forbidden lines such as [OII], [NII] relative to the Balmer emissions is stronger in collisional than in radiative. Actually these spectral feature highly depends on the physical state of ionized gas in both mechanisms, and moreover, the observations are quite incomplete in order to inspect their spectral feature. Nevertheless, the general feature of observation seems to be favorable for the collisional excitation mechanism.

Therefore, it may be useful to make a calculation from the view point of collisional excitation so as to give the wide variety of emission spectral feature as a function of physical state of gas (electron temperature T_e and electron density N_e). In this paper, a result of such a calculation is presented for the ranges of parameters: $T_e=1\sim10\times10^4$°K and $N_e=10^2\sim10^6$. Ionization degree and the effect of deactivation are both taken into consideration. In the calculation of PARKER (1964), where the parameters are taken in the range $T_e=1\sim10\times10^4$°K and $N_e=200\sim1{,}000$, the collisional ionization and excitation from the second energy level of hydrogen atom are not included. On the other hand, the calculation of BURBIDGE-GOULD-POTTASCH (1963) involves some over-simplification in the estimation of ionization degree, on which some remarks will be given later. In this way our present calculation may give a complement of the previous papers. The formulae will be summarized in Section 2 and the results will be given in Section 3. The last Section is devoted to some discussions.

In closing this section, we shall pay some attention to the evidence that the

emission spectra of the nuclei of galaxies seem to have some relationship with those of peculiar galaxies such as Seyfert galaxies (SEYFERT (1943), WOLTJER (1959)) and radio galaxies (e. g., SCHMIDT (1965)). Though the appearance of emission lines is generally much prevailing and much in variety in peculiar galaxies than in normal galaxies, the physical state of gases revealed by the emission spectra seems not so distinguished from each other in both types of galaxies. Moreover, in peculiar galaxies, the appearance of emission lines is usually supposed as an indication of violent activity occuring in their nuclei (e. g. BURBIDGE-BURBIDGE-SANDAGE (1963)). It is then not unreasonable to attribute the occurance of emissions in the normal galaxies to some violent activity, even its scale being much smaller. This problem is, however, beyond the scope of the present paper and will be discussed elsewhere.

2. Collision Spectrum: the formulae

In carrying out the calculation of collisional emission spectrum, we have made a selection of lines suitably from those usually observable in the nuclei of galaxies. They include following:

Balmer lines……$H_\alpha\lambda6563$, $H_\beta\lambda4862$, $H_\gamma\lambda4341$,

Forbidden lines……[OI] $\lambda\lambda6300+6364(^3P-^1D)$,

[OII] $\lambda\lambda3726+3728(^4S^\circ-^2D^\circ)$, [OIII] $\lambda\lambda5007+4959(^3P-^1D)$,

[NII] $\lambda\lambda6583+6548(^3P-^1D)$, [SII] $\lambda\lambda6716+6730(^4S^\circ-^2D^\circ)$,

[NeIII] $\lambda\lambda3868+3967(^3P-^1D)$, [NeV] $\lambda\lambda3425+3345(^3P-^1D)$.

The intensities of forbidden lines are computed for the total nebular transitions of atoms or ions above mentioned. These lines will be quoted hereafter as lines of [OI], [OII], and so on, without the indication of wave lengths.

(a) Balmer lines.

The hydrogen atom is simplified to have five discrete and one continuum energy levels. The intensities of Balmer lines $I_{2n}(n=3\sim5)$ are then given by, with the usual notations,

$$I_{2n}=N_nA_{n2}h\nu_{2n}, \qquad \cdots\cdots\cdots\cdots\cdots(2\cdot1)$$

where the population N_n of the n-th level is deduced from the cyclic equations, which are generally written as follows,

$$\sum_{n''>n}N_{n''}A_{n''n}+N_eN_e\alpha_{cn}+\sum_{n'=1}^{j}N_{n'}\beta_{n'n}=N_n\sum_{n'=j'}^{n-1}A_{nn'}, \qquad \cdots\cdots\cdots\cdots\cdots(2\cdot2)$$

$$(n\geq3;\ j,\ j'=1 \text{ or } 2)$$

where α_{cn} are the radiative recombination probabilities and $\beta_{n'n}$ are the probabilities of collisional excitation and ionization. Equation (2·2) gives the ionization formula when n is taken as c where c denotes the continuum level.

Since we have no concrete knowledge about optical depths of the ionized gas media for Lyman lines, we solve the cyclic equation (2·2) in the following three cases:

Case 1. The medium is optically thin for Lyman lines and collisional ionization and excitation take place only from the ground energy level. Then, we have $j=1$ and $j'=1$ in (2·2).

This case corresponds to Case A_2 of PARKER-MENZEL (1938).

Case 2a. The medium is optically thick for Lyman lines as in Case B of PARKER-MENZEL. The collisional upward transition also takes place from the ground level. Namely, we have $j=1$ and $j'=2$ in (2·2).

Case 2b. This is the same as Case 2a except taking into account the collisional upward transition from the second energy level. In This case we have $j=2$ and $j'=2$ in (2·2).

The selection of case would be made according to the optical depth of medium for L_α-radiation, τ_α, which is estimated and given in Table 1. $d\tau_\alpha/dz$ denotes the optical depth per one parsec.

Table 1. Optical depth of L_α radiation.

T_e In 10^4°K	$\frac{1}{N_e}\frac{d\tau_\alpha}{dz}$	
	Case 1, 2a	Case 2b
1.4	6.06(+5)	7.51(+3)
1.8	3.43(+4)	7.99(+2)
2.0	1.24(+4)	3.50(+2)
2.5	1.70(+3)	7.85(+1)
3.0	4.28(+2)	2.73(+1)
4.0	6.82(+1)	5.86(+0)

Note: The number in the parentheses in each column denote the power of 10.

The radii of the nuclei of galaxies are usually of the order of 100 pc, so that the total length of ionized gases in the line of sight would not be less than one parsec, even if high concentration of gas to a small volume is taken into account. Namely, ionized gas in nuclei may be sufficiently opaque in general, for Lyman lines as in Case 2, of which Case 2b may be more preferable than Case 2a.

The transition probabilities are adopted from the following source: Spontaneous transition $A_{n''n'}$……ALLEN (1955); radiative recombination α_{cn}……SEATON's (1959) formula in the first approximation; collisional ionization and excitation β_{jc}, β_{jn} ($j=1, 2$)……semiempirical data due to DE JAGER-KANNO-NEVEN (1960) and KANNO (unpublished).

(b) Forbidden lines.

The line intensity of each nebular line $I_{12}(X)$ for atom or ion X is given

$$I_{12}(X)=N_2A_{21}h\nu_{12}, \qquad \cdots\cdots\cdots\cdots\cdots\cdots(2\cdot3)$$

where N_2 is the population of the second metastable level and given as the solution of cyclic equations for the assumed three-level ion in the form,

$$\frac{N_2}{N_1}=\frac{\beta_{12}N_e}{A_{21}+\beta_{21}N_e}\left(1+\frac{1}{D}\frac{\beta_{13}}{\beta_{12}}\right), \qquad \cdots\cdots\cdots\cdots\cdots\cdots(2\cdot4)$$

where

$$D=1+\frac{A_{31}+\beta_{31}N_e}{A_{32}+\beta_{32}N_e}. \qquad \cdots\cdots\cdots\cdots\cdots\cdots(2\cdot5)$$

In deriving equation (2·4), we assumed that the collisional excitation takes place only from the ground level. Inserting (2·4) into (2·3) and making use of the collisional strength $\Omega(i, j)$, we can rewrite (2·3) in the form

$$I_{12}(X)=8.54\times10^{-6}h\nu_{12}\frac{N_eN_1(X)}{\sqrt{T_e}}A(X), \qquad \cdots\cdots\cdots\cdots\cdots\cdots(2\cdot6)$$

where

$$A(X)=\frac{\Omega(1,2)\exp\left(-\frac{E_{12}}{kT}\right)}{\tilde{\omega}_1\left(1+\frac{\beta_{21}}{A_{21}}N_e\right)}\left\{1+\frac{1}{D}\frac{\Omega(1,3)}{\Omega(1,2)}\exp\left[-\frac{E_{13}-E_{12}}{kT}\right]\right\}, \qquad \cdots\cdots\cdots(2\cdot7)$$

E_{ij} is the energy difference between i-th and j-th levels and $\tilde{\omega}_1$ is the statistical weight of the ground level.

The atomic data for the forbidden lines are adopted from the following sources: the transition probabilities A_{ij}……SEATON (1955) for N, O, S, and GARSTANG (1951, 1960) for Ne; the collision strengths $\Omega(i, j)$……SEATON (1958).

(c) Relative intensities.

The relative line intensities are easily computed when the relative abundbnce and the degree of ionization are given. In this paper we adopt the relative abundance of GOLDBERG-MULLER-ALLER (1960) for the sun, except neon, for which the abundance for stars in the same reference is taken. In this way we assume in the relative number density

$$\log \mathbf{H}=12,\ \log \mathbf{N}=7.98,\ \log \mathbf{O}=8.96,\ \log \mathbf{Ne}=8.90 \text{ and } \log \mathbf{S}=7.30.$$

As for the ionization formula, we make use of the expression due to PARKER (1964), which is ELWERT's (1952) ionization formula for hydrogen-like atom with the fitting constant C by PARKER and is given as

$$\frac{N(X^+)}{N(X)}=C\frac{\zeta_n}{n_{\frac{1}{2}}}\left(\frac{x_n}{x_H}\right)^{-2}\left(\frac{x_n}{kT}\right)^{-1}\exp\left(-\frac{x_n}{kT}\right), \qquad \cdots\cdots\cdots\cdots\cdots\cdots(2\cdot8)$$

where

$$C=2.7\times10^5,$$

ζ_n is the number of electrons in the outermost shell, n, of the atom or ion X and hydrogen, respectively.

3. Collision spectrum: the results

The relative intensities for some pairs of emission lines computed with the aide of the formulae given above are summarized in this section. The values of intensities are expressed with the power of 10, whose exponents are given in the parentheses after the figures in Tables 3 to 11.

(1) Balmer decrement. The decrement is calculated in Cases 1, 2a and 2b

Table 2. Collisional Balmer decrement

T_e	Case 1			Case 2a			Case 2b		
in 10^4°K	H_α	H_β	H_γ	H_α	H_β	H_γ	H_α	H_β	H_γ
1.0	6.35	1.00	0.314	8.34	1.00	0.268	18.80	1.00	0.207
1.2	5.47	1.00	0.333	7.27	1.00	0.285	15.55	1.00	0.227
1.4	5.02	1.00	0.347	6.68	1.00	0.295	14.07	1.00	0.233
1.6	4.69	1.00	0.356	6.23	1.00	0.303	13.19	1.00	0.244
1.8	4.50	1.00	0.362	5.98	1.00	0.308	12.49	1.00	0.251
2.0	4.30	1.00	0.366	5.75	1.00	0.311	11.97	1.00	0.257
2.2	4.03	1.00	0.370	5.41	1.00	0.314	11.41	1.00	0.261
2.5	3.89	1.00	0.374	5.24	1.00	0.318	10.76	1.00	0.265
3.0	3.75	1.00	0.380	5.06	1.00	0.322	10.01	1.00	0.270
3.5	3.60	1.00	0.384	4.86	1.00	0.326	9.52	1.00	0.275
4.0	3.52	1.00	0.387	4.78	1.00	0.329	9.01	1.00	0.278
5.0	3.38	1.00	0.393	4.60	1.00	0.333	8.62	1.00	0.283
6.0	3.32	1.00	0.397	4.52	1.00	0.337	8.27	1.00	0.286
7.0	3.24	1.00	0.400	4.43	1.00	0.339	8.09	1.00	0.288
8.0	3.22	1.00	0.403	4.40	1.00	0.342	7.90	1.00	0.290
9.0	3.21	1.00	0.406	4.39	1.00	0.343	7.77	1.00	0.291
10.0	3.20	1.00	0.409	4.38	1.00	0.345	7.65	1.00	0.293

Table 3-1. Relative intensity of H_α/[NII] in Case 1.

T_e \ N_e	10^2
10^4°K	
1.0	4.89(+0)
1.2	1.62(+0)
1.4	9.33(−1)
1.6	5.33(−1)
1.8	3.63(−1)
2.0	2.75(−1)
2.2	2.05(−1)
2.5	1.58(−1)
3.0	1.17(−1)
3.5	1.15(−1)
4.0	1.52(−1)
5.0	4.69(−1)
6.0	1.41(+0)
7.0	3.93(+0)
8.0	1.10(+1)
9.0	3.05(+1)

Table 3-2. Relative intensity of H_α/[NII] in Case 2a.

T_e \ N_e	10^2	10^3	10^4	10^5	10^6
10^4°K					
1.0	1.16(+1)	1.17(+1)	1.27(+1)	2.24(+1)	1.19(+2)
1.2	3.89(+0)	3.92(+0)	4.22(+0)	7.18(+0)	3.68(+1)
1.4	2.25(+0)	2.27(+0)	2.42(+0)	3.74(+0)	1.98(+1)
1.6	1.29(+0)	1.30(+0)	1.39(+0)	2.24(+0)	1.077(+1)
1.8	8.82(−1)	8.87(−1)	9.41(−1)	1.49(+0)	6.97(+0)
2.0	6.71(−1)	6.74(−1)	7.14(−1)	1.11(+0)	5.08(+0)
2.2	5.31(−1)	5.34(−1)	5.64(−1)	8.61(−1)	3.84(+0)
2.5	3.87(−1)	3.89(−1)	4.10(−1)	6.14(−1)	2.66(+0)
3.0	2.89(−1)	2.90(−1)	3.05(−1)	4.44(−1)	1.84(+0)
3.5	2.83(−1)	2.84(−1)	2.97(−1)	4.23(−1)	1.68(+0)
4.0	3.72(−1)	3.73(−1)	3.88(−1)	5.43(−1)	2.09(+0)
5.0	1.14(+0)	1.15(+0)	1.19(+0)	1.62(+0)	5.88(+0)
6.0	3.44(+0)	3.45(+0)	3.57(+0)	4.74(+0)	1.65(+1)
7.0	9.71(+0)	9.74(+0)	1.004(+1)	1.31(+1)	4.37(+1)
8.0	2.68(+1)	2.68(+1)	2.76(+1)	3.55(+1)	1.14(+2)
9.0	7.15(+1)	7.15(+1)	4.50(+1)	5.80(+1)	2.90(+2)

Table 3-3. Relative intensity of H_α/[NII] in Case 2b.

T_e \ N_e	10^2	10^3	10^4	10^5	10^6
10^4°K					
1.0	6.52(+3)	6.57(+3)	7.11(+3)	1.26(+4)	6.70(+4)
1.2	2.98(+2)	3.01(+2)	3.23(+2)	5.50(+2)	2.82(+3)
1.4	2.75(+1)	2.77(+1)	2.96(+1)	4.57(+1)	2.43(+2)
1.6	5.76(+0)	5.79(+0)	6.18(+0)	9.96(+0)	4.79(+1)
1.8	2.54(+0)	2.56(+0)	2.71(+0)	4.29(+0)	2.01(+1)
2.0	1.66(+0)	1.67(+0)	1.76(+0)	2.74(+0)	1.26(+1)
2.2	1.29(+0)	1.30(+0)	1.33(+0)	2.04(+0)	9.07(+0)
2.5	9.14(−1)	9.19(−1)	9.67(−1)	1.45(+0)	6.28(+0)
3.0	6.59(−1)	6.62(−1)	6.94(−1)	1.01(+0)	4.18(+0)
3.5	6.43(−1)	6.45(−1)	6.74(−1)	9.60(−1)	3.82(+0)
4.0	8.17(−1)	8.20(−1)	8.54(−1)	1.19(+0)	4.61(+0)
5.0	2.63(+0)	2.64(+0)	2.74(+0)	3.72(+0)	1.35(+1)
6.0	7.94(+0)	7.97(+0)	8.26(+0)	1.09(+1)	3.80(+1)
7.0	2.35(+1)	2.36(+1)	2.43(+1)	3.17(+1)	1.058(+2)
8.0	6.69(+1)	6.71(+1)	6.90(+1)	8.88(+1)	2.86(+2)
9.0	1.86(+2)	1.88(+2)	1.90(+2)	2.48(+2)	7.50(+2)

Table 4-1. Relative intensity of H_α/[OII] in Case 1.

T_e \ N_e	10^2
10^4°K	
1.0	2.42(−1)
1.2	7.88(−2)
1.4	5.03(−2)
1.6	4.08(−2)
1.8	3.26(−2)
2.0	2.49(−2)
2.2	1.76(−2)
2.5	1.25(−2)
3.0	7.89(−3)
3.5	5.67(−3)
4.0	5.08(−3)
5.0	8.30(−3)
6.0	2.19(−2)
7.0	5.57(−2)
8.0	1.48(−1)
9.0	4.00(−1)

Table 4-2. Relative intensity of H_α/[OII] in Case 2a.

T_e \ N_e	10^2	10^3	10^4	10^5	10^6
10^4°K					
1.0	5.78(−1)	6.50(−1)	1.38(+0)	8.65(+0)	8.13(+1)
1.2	1.89(−1)	2.11(−1)	4.29(−1)	2.61(+0)	2.44(+1)
1.4	1.21(−1)	1.34(−1)	2.64(−1)	1.56(+0)	1.45(+1)
1.6	9.89(−2)	1.089(−1)	2.08(−1)	1.20(+0)	1.11(+1)
1.8	7.93(−2)	8.66(−2)	1.61(−1)	9.06(−1)	8.35(+0)
2.0	6.06(−2)	6.60(−2)	1.20(−1)	6.61(−1)	6.06(+0)
2.2	4.57(−2)	4.96(−2)	8.84(−2)	4.77(−1)	4.35(+0)
2.5	3.06(−2)	3.31(−2)	5.76(−2)	3.03(−1)	2.76(+0)
3.0	1.95(−2)	2.09(−2)	3.51(−2)	1.77(−1)	1.60(+0)
3.5	1.41(−2)	1.50(−2)	2.45(−2)	1.20(−1)	1.069(+0)
4.0	1.24(−2)	1.32(−2)	2.10(−2)	9.91(−2)	8.83(−1)
5.0	2.03(−2)	2.14(−2)	3.29(−2)	1.48(−1)	1.29(+0)
6.0	5.34(−2)	5.62(−2)	8.40(−2)	3.61(−1)	3.13(+0)
7.0	1.37(−1)	1.44(−1)	2.10(−1)	8.68(−1)	7.43(+0)
8.0	3.61(−1)	3.77(−1)	5.41(−1)	2.16(+0)	1.84(+1)
9.0	9.22(−1)	9.80(−1)	1.33(+0)	5.20(+0)	4.65(+1)

Table 4-3. Relative intensity of H_α/[OII] in Case 2b.

T_e \ N_e	10^2	10^3	10^4	10^5	10^6
10^4°K					
1.0	3.24(+2)	3.65(+2)	7.73(+2)	4.85(+3)	4.57(+4)
1.2	1.45(+1)	1.62(+1)	3.23(+1)	2.00(+2)	1.87(+3)
1.4	1.48(+0)	1.64(+0)	3.22(+0)	1.90(+1)	1.77(+2)
1.6	4.40(−1)	4.85(−1)	9.24(−1)	5.32(+0)	4.92(+1)
1.8	2.28(−1)	2.50(−1)	4.64(−1)	2.61(+0)	2.40(+1)
2.0	1.50(−1)	1.63(−1)	2.96(−1)	1.63(+0)	1.50(+1)
2.2	1.11(−1)	1.21(−1)	2.09(−1)	1.12(+0)	1.028(+1)
2.5	7.23(−2)	7.81(−2)	1.36(−1)	7.14(−1)	6.49(+0)
3.0	4.44(−2)	4.77(−2)	8.01(−2)	4.05(−1)	3.65(+0)
3.5	3.20(−2)	3.41(−2)	5.57(−2)	2.72(−1)	2.42(+0)
4.0	2.72(−2)	2.89(−2)	4.62(−2)	2.19(−1)	1.94(+0)
5.0	4.66(−2)	4.92(−.)	7.54(−2)	3.40(−1)	2.98(+0)
6.0	1.23(−2)	1.30(−1)	1.94(−1)	8.34(−1)	7.21(+0)
7.0	3,32(−1)	3.48(−1)	5.07(−1)	2.10(+0)	1.80(+1)
8.0	9.03(−1)	9.43(−1)	1.35(+0)	5.40(+0)	4.59(+1)
9.0	2.40(+0)	2.57(+0)	3.58(+0)	1.40(+1)	1.15(+2)

Table 5-1. Relative intensity of H_α/[OIII] in Case 1.

T_e \ N_e	10^2
10^4°K	
2.0	9.80(+3)
2.2	1.031(+3)
2.5	7.38(+1)
3.0	2.76(+0)
3.5	2.59(−1)
4.0	4.94(−2)
5.0	8.97(−3)
6.0	5.22(−3)
8.0	5.13(−3)
10.0	4.54(−3)

Table 5-2. Relative intensity of H_α/[OIII] in Case 2a.

T_e \ N_e	10^2	10^3	10^4	10^5	10^6
10^4°K					
2.0	2.39(+4)	2.39(+4)	2.41(+4)	2.55(+4)	4.02(+4)
2.2	2.68(+3)	2.68(+3)	2.70(+3)	2.86(+3)	4.43(+3)
2.5	1.81(+2)	1.81(+2)	1.82(+2)	1.92(+2)	2.92(+2)
3.0	6.82(+0)	6.82(+0)	6.85(+0)	7.20(+0)	1.062(+1)
3.5	6.43(−1)	6.43(−1)	6.46(−1)	6.76(−1)	9.75(−1)
4.0	1.21(−1)	1.21(−1)	1.21(−1)	1.26(−1)	1.79(−1)
5.0	2.19(−2)	2.19(−2)	2.20(−2)	2.29(−2)	3.13(−2)
6.0	1.27(−2)	1.27(−2)	1.28(−2)	1.32(−2)	1.78(−2)
8.0	1.25(−2)	1.25(−2)	1.26(−2)	1.29(−2)	1.68(−2)
10.0	1.11(−2)	1.11(−2)	1.11(−2)	1.14(−2)	1.14(−2)

Table 5-3. Relative intensity of H_α/[OIII] in Case 2b.

T_e \ N_e	10^2	10^3	10^4	10^5	10^6
10^4°K					
2.0	5.91(+4)	5.91(+4)	5.95(+4)	6.32(+4)	9.94(+4)
2.2	6.51(+3)	6.52(+3)	6.36(+3)	6.75(+3)	1.044(+4)
2.5	4.27(+2)	4.27(+2)	4.30(+2)	4.54(+2)	6.89(+2)
3.0	1.55(+1)	1.55(+1)	1.56(+1)	1.64(+1)	2.42(+1)
3.5	1.46(+0)	1.46(+0)	1.47(+0)	1.53(+0)	2.21(+0)
4.0	2.65(−1)	2.65(−1)	2.66(−1)	2.78(−1)	3.93(−1)
5.0	5.03(−2)	5.04(−2)	5.05(−2)	5.26(−2)	7.21(−2)
6.0	2.94(−2)	2.94(−2)	2.96(−2)	3.06(−2)	4.11(−2)
8.0	3.13(−2)	3.13(−2)	3.14(−2)	3.24(−2)	4.20(−2)
10.0	3.02(−2)	3.02(−2)	3.02(−2)	3.11(−2)	3.95(−2)

and shown in Table 2 and Figure 1.

(2) H_α versus forbidden line intensities. The relative intensities of H_α relative to [NII], [OII], and [OIII] are calculated for the whole range of parameters T_e and N_e in Cases 2a and b of Balmer lines, while only for $N_e=10^2$ in Case 1. They are given in Tables 3 to 5.

(3) Relative intensities of forbidden lines. The relative intensities for the following pairs of forbidden lines are calculated: [OII]/[OI], [OIII]/[OII],

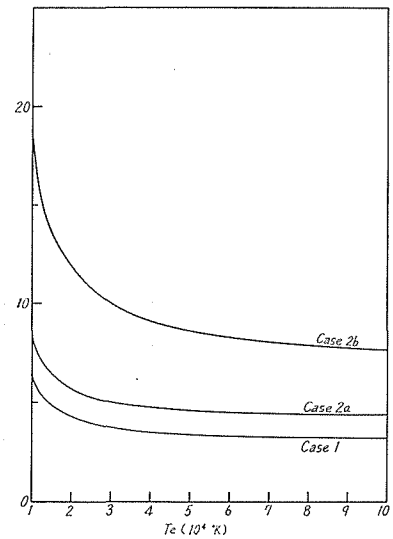

Fig. 1. Temperature dependence of Balmer decrement H_α: H_β.

Table 6. Relative intensity of [OII]/[OI].

T_e \ N_e	10^2	10^3	10^4	10^5	10^6
10^4°K					
0.9	1.74(−3)	1.54(−3)	7.13(−4)	1.19(−4)	2.01(−5)
1.0	1.23(−2)	1.089(−2)	5.18(−3)	8.79(−4)	2.10(−4)
1.1	6.17(−2)	5.51(−2)	2.68(−2)	4.64(−3)	8.06(−4)
1.2	2.36(−1)	2.12(−1)	1.048(−1)	1.84(−2)	3.24(−3)
1.4	2.00(+0)	1.81(+0)	9.26(−1)	1.68(−1)	3.01(−2)
1.6	9.74(+0)	8.86(+0)	4.68(+0)	8.73(−1)	1.59(−1)
1.8	3.42(+1)	3.13(+1)	1.69(+1)	3.24(+0)	5.94(−1)
2.0	9.35(+1)	8.60(+1)	4.76(+1)	9.29(+0)	1.73(+0)
2.5	5.93(+2)	5.50(+2)	3.18(+2)	6.52(+1)	1.23(+1)
3.0	2.04(+3)	1.94(+3)	1.16(+3)	2.48(+2)	4.71(+1)
3.5	5.18(+3)	4.86(+3)	3.00(+3)	6.63(+2)	1.27(+2)
4.0	1.044(+4)	9.82(+3)	6.20(+3)	1.41(+3)	2.71(+2)

Table 7. Relative intensity of [OIII]/[OII].

T_e \ N_e	10^2	10^3	10^4	10^5	10^6
10^4°K					
2.0	2.56(−6)	2.79(−6)	5.05(−6)	2.62(−5)	1.52(−4)
2.2	1.71(−5)	1.85(−5)	3.28(−5)	1.67(−4)	9.85(−4)
2.5	1.69(−4)	1.82(−4)	3.15(−4)	1.57(−3)	9.40(−3)
3.0	2.91(−3)	3.06(−3)	5.12(−3)	2.46(−2)	1.50(−1)
3.5	2.19(−2)	2.33(−2)	3.79(−2)	1.77(−1)	1.095(+0)
4.0	1.027(−1)	1.092(−1)	1.74(−1)	7.87(−1)	4.94(+0)
5.0	9.32(−1)	9.85(−1)	1.51(+0)	6.52(+0)	4.16(+1)
6.0	4.19(+0)	4.41(+0)	6.55(+0)	2.72(+1)	1.76(+2)
7.0	1.26(+1)	1.31(+1)	1.91(+1)	7.64(+1)	4.98(+2)
8.0	2.91(+1)	3.04(+1)	4.33(+1)	1.68(+2)	1.10(+3)
9.0	5.68(+1)	5.92(+1)	8.30(+1)	3.14(+2)	2.06(+3)
10.0	9.81(+1)	1.020(+2)	1.41(+2)	5.20(+2)	3.43(+3)

Table 8. Relative intensity of [NII]/[OII].

T_e \ N_e	10^2	10^3	10^4	10^5	10^6
10^4°K					
1.0	4.98(−2)	5.56(−2)	1.087(−1)	3.87(−1)	6.83(−1)
1.2	4.87(−2)	5.39(−2)	1.018(−1)	3.64(−1)	6.63(−1)
1.4	5.40(−2)	5.93(−2)	1.089(−1)	4.17(−1)	7.30(−1)
1.6	7.65(−2)	8.37(−2)	1.50(−1)	5.34(−1)	1.028(+0)
1.8	8.99(−2)	9.78(−2)	1.71(−1)	6.09(−1)	1.20(+0)
2.0	9.03(−2)	9.78(−2)	1.68(−1)	5.96(−1)	1.19(+0)
2.2	8.62(−2)	9.30(−2)	1.57(−1)	5.54(−1)	1.13(+0)
2.5	7.92(−2)	8.51(−2)	1.41(−1)	4.93(−1)	1.036(+0)
3.0	6.88(−2)	7.20(−2)	1.16(−1)	4.01(−1)	8.73(−1)
3.5	4.98(−2)	5.29(−2)	8.26(−2)	2.83(−1)	6.35(−1)
4.0	3.30(−2)	3.49(−2)	5.35(−2)	1.81(−1)	4.17(−1)
5.0	1.77(−2)	1.87(−2)	2.77(−2)	9.14(−2)	2.20(−1)
6.0	1.56(−2)	1.63(−2)	2.35(−2)	7.62(−2)	1.90(−1)
7.0	1.42(−2)	1.48(−2)	2.14(−2)	6.62(−2)	1.70(−1)
8.0	1.35(−2)	1.41(−2)	1.96(−2)	6.09(−2)	1.61(−1)

Table 9. Relative intensity of [SII]/[OII].

T_e \ N_e	10^2	10^3	10^4	10^5	10^6
10^4°K					
0.9	1.21(+1)	1.35(+1)	2.55(+1)	7.06(+1)	1.002(+2)
1.0	5.52(+0)	6.13(+0)	1.14(+1)	3.17(+1)	4.56(+1)
1.1	2.14(+0)	2.36(+0)	4.31(+0)	1.21(+1)	1.77(+1)
1.2	7.95(−1)	8.75(−1)	1.57(+0)	4.44(+0)	6.55(+0)
1.4	1.56(−1)	1.70(−1)	2.98(−1)	8.47(−1)	1.28(+0)
1.6	7.19(−2)	7.82(−2)	1.34(−1)	3.83(−1)	5.89(−1)
1.8	5.21(−2)	5.65(−2)	9.49(−2)	2.72(−1)	4.25(−1)
2.0	4.42(−2)	4.76(−2)	7.86(−2)	2.26(−1)	3.59(−1)
2.2	3.89(−2)	4.18(−2)	6.79(−2)	1.95(−1)	3.14(−1)
2.5	3.09(−2)	3.30(−2)	5.27(−2)	1.51(−1)	2.49(−1)
3.0	1.48(−2)	1.54(−2)	2.39(−2)	6.85(−2)	1.16(−1)
3.5	4.87(−3)	5.15(−3)	7.82(−3)	2.22(−2)	3.87(−2)
4.0	1.82(−3)	1.92(−3)	2.86(−3)	8.10(−3)	1.44(−2)

Table 10. Relative intensity of [NeIII]/[OIII].

N_e \ T_e	10^2	10^3	10^4	10^5	10^6
10^4°K					
3	4.75(−2)	4.75(−2)	4.77(−2)	5.00(−2)	7.19(−2)
4	1.43(−1)	1.43(−1)	1.43(−1)	1.49(−1)	2.06(−1)
5	3.75(−1)	3.75(−1)	3.77(−1)	3.90(−1)	5.25(−1)
6	3.32(−1)	3.32(−1)	3.34(−1)	3.45(−1)	4.54(−1)
7	6.55(−1)	6.55(−1)	6.57(−1)	6.78(−1)	8.78(−1)
8	9.03(−1)	9.03(−1)	9.06(−1)	9.32(−1)	1.19(+0)
9	1.063(+0)	1.064(+0)	1.066(+0)	1.095(+0)	1.38(+0)
10	2.54(+0)	2.55(+0)	2.55(+0)	2.62(+0)	3.27(+0)

Table 11. Relative intensity of [NeV]/[NeIII].

T_e \ N_e	10^2	10^3	10^4	10^5	10^6
10^4°K					
7	3.69(−6)	3.69(−6)	3.69(−6)	3.70(−6)	3.73(−6)
8	1.37(−4)	1.37(−4)	1.37(−4)	1.37(−4)	1.38(−4)
9	2.32(−3)	2.32(−3)	2.32(−3)	2.33(−3)	2.34(−3)
10	2.30(−2)	2.29(−2)	2.30(−2)	2.30(−2)	2.31(−2)

[NII]/[OII], [SII]/[OII], [NeIII]/[OIII], and [NeV]/[NeIII]. The results are shown in Tables 6∼11.

(4) Iso-intensity curves on the (T_e-N_e) diagram. The relative intensities given in Table 3∼11 can be conveniently expressed as the iso-intensity curves on the (T_e-N_e) diagram. They are shown separately in two figures in order to avoid the complexity of drawing.

(5) Theoretical collision spectrum. With the aide of Tables 3∼11, we can also compose the theoretical collision spectrum which are shown in Table 12 for lower part ($T_e=1\sim5\times10^4$°K) and in Table 13 for higher part ($T_e=4\sim10\times10^4$°K),

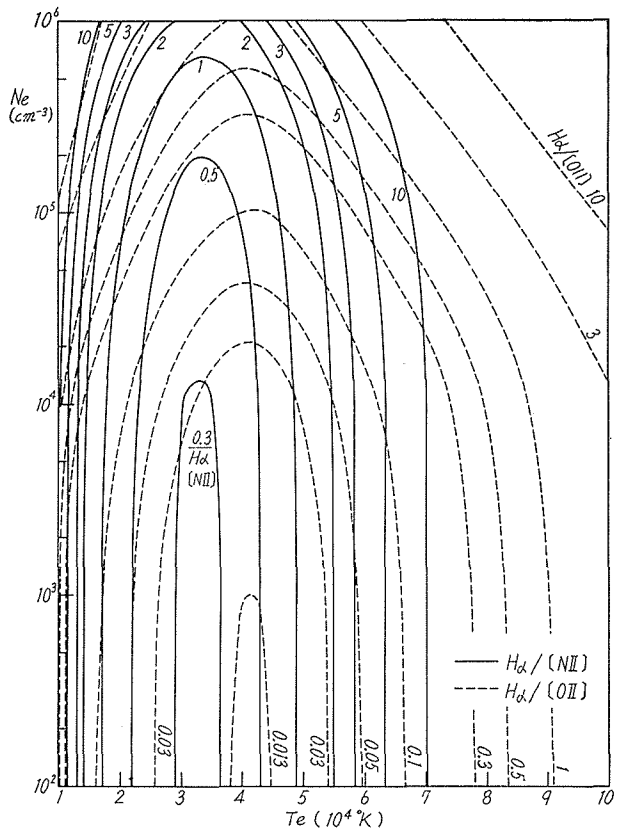

Fig. 2a. Iso-intensity curves on T_e-N_e diagram.
(Relative intensities including H_α in Case 2a.)

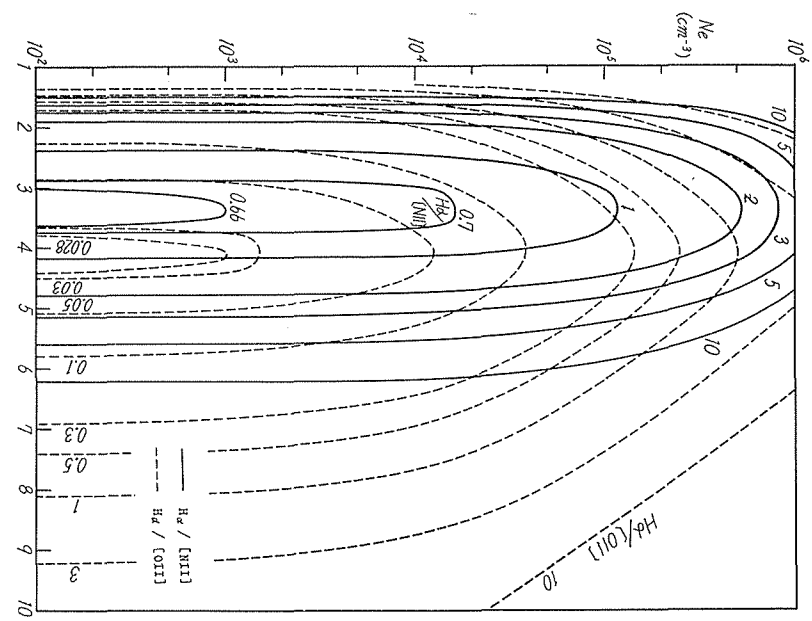

Fig 2b. Iso-intensity curves on ($T_e - N_e$) diagram.
(Relative intensities including H_α in Case 2b)

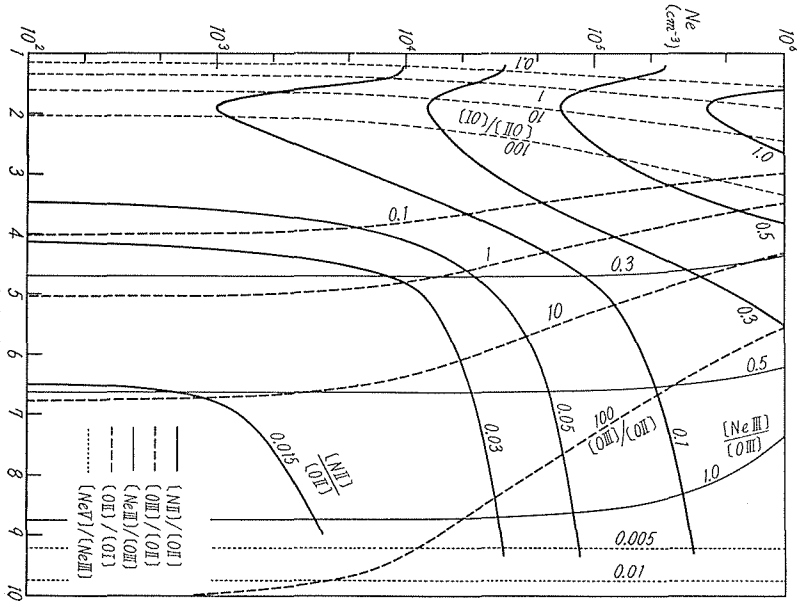

Fig. 3. Iso-intensity curves on ($T_e - N_e$) diagram.
(Relative forbidden line intensities)

Table 12 Theoretical collision spectrum in the range of $T_e=1\sim5\times10^4$°K, in unit of [OII]=10.

N_e	T_e in 10^4°K	[OII] λλ3726 +3728	[NeIII] λλ3868 +3967	[OIII] λλ5007 +4959	[OI] λλ6300 +6364	H_α case 2b λ6563	[NII] λλ6583 +6548	[SII] λλ6716 +6730
10^2	1	10	—	—	816.00	3.24×10^3	0.50	552.00
	2	10	—	—	0.11	1.50	0.90	0.44
	3	10	—	0.03	0.01	0.44	0.69	0.15
	4	10	0.15	1.03	—	0.27	0.33	0.02
	5	10	3.50	9.32	—	0.47	0.18	—
10^3	1	10	—	—	918.00	3.65×10^3	0.56	613.00
	2	10	—	—	0.12	1.63	0.98	0.48
	3	10	—	0.03	0.01	0.48	0.72	0.15
	4	10	0.15	1.09	—	0.29	0.35	0.02
	5	10	3.69	9.85	—	0.49	0.19	—
10^4	1	10	—	—	1.93×10^3	7.73×10^3	1.09	1.14×10^3
	2	10	—	—	0.21	2.96	1.68	0.79
	3	10	—	0.05	0.01	0.80	1.16	0.24
	4	10	0.25	1.74	—	0.46	0.54	0.03
	5	10	5.69	15.10	—	0.75	0.28	—
10^5	1	10	—	—	1.14×10^4	4.85×10^4	3.87	3.17×10^3
	2	10	—	—	1.08	16.30	5.96	2.26
	3	10	0.01	0.25	0.04	4.05	4.01	0.69
	4	10	1.17	7.87	0.01	2.19	1.81	0.08
	5	10	25.40	65.20	—	3.40	0.91	—
10^6	1	10	—	—	4.76×10^4	4.57×10^5	6.83	4.56×10^3
	2	10	—	—	5.80	150.00	11.90	3.59
	3	10	0.11	1.50	0.21	36.50	8.73	1.16
	4	10	10.20	49.40	0.04	19.40	4.17	0.14
	5	10	218.00	416.00	0.01	29.80	2.20	—

separately. The unit of intensity is taken as [OII]=10 in Table 12 and [OIII]=10 in Table 13.

(6) Gross feature of collision spectrum. Because of the low dispersion spectroscopy for most of galaxies, and because of the situation that emission lines are generally superposed on the strong background spectra, it is quite difficult to measure the reliable relative intensities of emission lines. For most galaxies, observable lines are limited to some strong ones, and, moreover, their relative intensities are usually denoted by the specification of equality or inequality, as shown in Table A2. It is therefore rather convenient to compose the gross feature of collision spectrum and to compare them with observations. For this purpose, we adopt the five lines of [H_α], [OI], [OII], [OIII], and [NII], and classify the type of collision spectra as follows, according to their relative intensities:

Type	Relative intensities
O	[OII]≫Any of ([OI], [OIII], [NII], H_α)
ONB~ON	[OII]>Any of ([OIII], [OI], [NII], H_α), [NII]≳H_α
OBN	[OII]>Any of ([OIII], [OI]), [OII]≳H_α≳[NII]
B~BN	H_α≳[NII]>[OII]>Any of ([OI], [OIII])
HO	[OIII]≳[OII]≫[OI], [OII]>Any of (H_α, [NII])

Table 13 Theoretical collision spectrum in the range of $T_e=4\sim10\times10^{4\circ}K$, in unit of [OIII]=10.

N_e	T_e in $10^{4\circ}K$	[NeV] λλ3425 +3345	[OII] λλ3726 +3728	[NeIII] λλ3868 +3967	[OIII] λλ5007 +4959	H_α case 2b λ6563	[NII] λλ6583 +6548
	4	—	97.40	1.43	10	2.65	3.21
	5	—	10.70	3.75	10	0.50	0.19
	6	—	2.39	3.32	10	0.29	0.04
10^2	7	—	0.79	6.55	10	0.27	0.01
	8	—	0.34	9.03	10	0.31	0.01
	9	0.03	0.18	10.60	10	0.46	—
	10	0.58	0.10	25.40	10	—	—
	4	—	91.60	1.43	10	2.65	3.20
	5	—	10.20	3.75	10	0.50	0.19
	6	—	2.27	3.32	10	0.29	0.04
10^3	7	—	0.76	6.55	10	0.27	0.01
	8	—	0.33	9.03	10	0.31	0.01
	9	0.03	0.17	10.60	10	0.46	—
	10	0.58	0.10	25.50	10	—	—
	4	—	57.50	1.43	10	2.66	3.07
	5	—	6.62	3.77	10	0.51	0.18
	6	—	1.53	3.34	10	0.30	0.04
10^4	7	—	0.52	6.57	10	0.27	0.01
	8	—	0.23	9.06	10	0.31	0.01
	9	0.03	0.12	10.70	10	0.46	—
	10	0.59	0.07	25.50	10	—	—
	4	—	12.70	1.49	10	2.78	2.30
	5	—	1.53	3.90	10	0.53	0.14
	6	—	0.37	3.45	10	0.31	0.03
10^5	7	—	0.13	6.78	10	0.27	0.01
	8	—	0.06	9.32	10	0.32	—
	9	0.03	0.03	11.00	10	0.48	—
	10	0.06	0.02	26.20	10	—	—
	4	—	2.02	2.06	10	3.39	0.84
	5	—	0.24	5.25	10	0.72	0.05
	6	—	0.06	4.54	10	0.41	0.01
10^6	7	—	0.02	8.78	10	0.36	—
	8	—	0.01	11.90	10	0.42	—
	9	0.03	0.01	13.80	10	0.61	—
	10	0.76	—	32.70	10	—	—

HOBN [OIII] $\gtrsim$ [OII] $\gg$ [OI],
[OII] $\gtrsim H_\alpha \gtrsim$ [NII]

HBON [OIII] $\gtrsim$ [OII] $\gg$ [OI],
$H_\alpha \gtrsim$ [OII] $\gtrsim$ [NII]

The symbol **H** is used in the sense of "higher excitation" in the spectrum. In expressing the relative intensities, the inequality symbols denote the following relation;

A $\gg$ B……when A is more than 10 times stronger than B,
A $>$ B……when A is more than 3 times stronger than B,
A $\gtrsim$ B……when A is nearly equal to or stronger than B.

The regions which the spectrum of each type of relative intensities should occupy on the (N_e-T_e) diagram are schematically shown in Fig. 4. The translation from one type to another is quite graduate, so that the typical spectrum of each type would be visualized in the central part of each region given in Fig. 4.

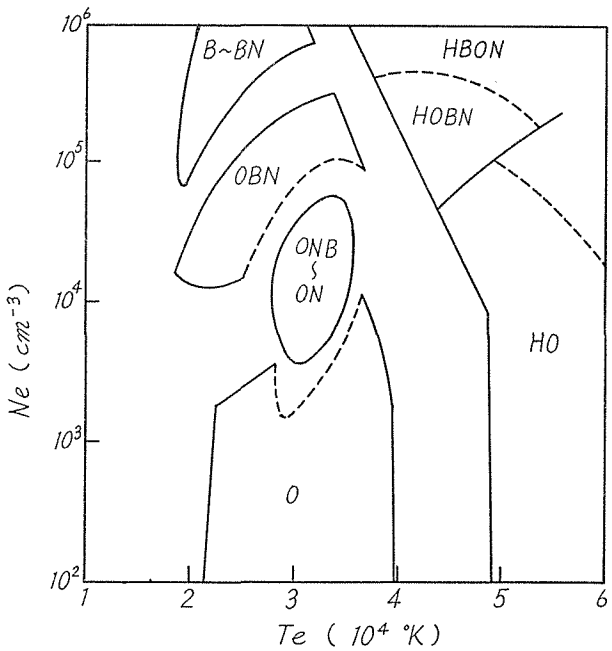

Fig. 4. Schematic diagram showing the regions of same gross feature in the collision spectrum. The notations are explained in the text; Section 3, article (6).

4. Discussions.

a) General feature of collision spectrum.

The general feature of collision spectrum described by MINKOWSKY (1955), MIYAMOTO (1956) and recently by PARKER (1964) is generally confirmed, but much sensitive dependence upon the physical state of gas is emphasized.

First, the Balmer decrement given in Table 2 may be in good agreement with the previous calculations due to CHAMBERLAIN (1953) and PARKER (1964) in Cases 1 and 2a. In comparison with these decrements, the decrement in Case 2b is remarkably steep. This evidently shows that the collisional excitation from the second energy level contributes to the increase of populations of lower energy levels relative to higher ones. Of Cases 1, 2a, and 2b, Case 1 may be excluded from the present consideration by the reason mentioned in Section 2, and Case 2a implicitly involves a physically inconsistent process in the condition of statistical equilibrium for the second energy level, namely electrons entered into the second level could not leave there without violating the system of the cyclic equations. Although the calculations have so far been made on the basis of Case 1 or 2a, we suppose that Case 2b is more self-consistent and reasonable so far as the nebula is sufficiently opaque for Lyman alpha radiation.

Second, the weak intensity of Balmer lines relative to forbidden lines, which has been previously emphasized as an another characteristic of collision spectrum, is also presented in our calculation, especially in the region of low electron density. For Example, H_α/[OII] ratio is less than unity when $N_e=10$ in the moderate

temperatures about 20,000°K. For dense nebulae, however, the intensity of H_α becomes high, so that the discrimination between radiative and collisional spectrum becomes difficult. The density dependence of relative intensities can also be seen in some relative intensities of forbidden lines, of which the ratio [NII]/[OII] remarkably changes its value as shown in Fig. 3.

Besides, it should be noticed that relative intensities between different kinds of elements can vary fairly sensitively according to its relative abundance. The general feature of collision spectrum described here, however, might not suffer serious change due to the abundance ratios.

b) Physical state of ionized gas in the nuclei of galaxies.

If one may suppose that the emission spectra of the nuclei of galaxies are formed by collisional excitation, the diversity of galaxies in the relative intensities of emission lines could be explained by the variety of physical state of ionized gas. Namely, if the observed emission spectra which are compiled in the Appendix can be well within the predicted collision spectra given as the type of gross feature in the preceding section, one can guess that the emission mechanism in the nuclei is of collisional character, and this, in turn, enable us to estimate the physical state of ionized gases there.

The comparison between theory and observation may be conveniently made in the following form:

Observation (Table A2) Group (Subgroup)		Theory Type of collision Spectra
1	(OII)	**O**
2	(OII>N)	**ON**
	(OII<N)	—
3	(OII>N>α)	**ONB**
	(OII≲N∼α)	**B** or **BN**
	(OII≲N<α)	**B** or **BN**
	(OII∼α>N)	**OBN**
4	(OII<α)	—
5	(N≲α)	**B** or **BN**
	(N>α)	(**BN**)

The subgroups of Table A2 in which the relative intensities among H_α, [OII], and [NII] are not given, are omitted from the above comparison. Furthermore we also excluded the galaxies in which [OIII]-line is stronger than [OII]-lines, since those galaxies are small in number among normal galaxies and, in addition, the theoretical spectra are somewhat uncertain in the temperature region higher than 4 or 5×10^4°K as shown later. The comparison is made for the remaining galaxies.

The correspondence is, as shown above, not complete: for example, there is no type of theoretical spectrum which corresponds to the subgroup 2 (OII<N) or 4 (OII<α). Nevertheless if we take into account the ambiguity of observed emission spectra, the accordance may be rather satisfactory.

On the basis of collision spectrum, the physical state of ionized gas can be determined from the above correspondence table and Fig. 4, according to which the wide range of electron density is quite remarkable: The galaxies classified as group 1 in Table A2 indicate the electron density lower than $\sim10^3$cm^{-3}, where as the

galaxies in Group 5 ([OII] is much weaker than any of H_α and [NII]) show the electron density as high as $10^5 \sim 10^6 cm^{-3}$. In Table A2, it may be also interesting to notice a general correlation that the galaxies in earlier morphological types mainly belong to earlier grouping (Groups 1~2), whereas the galaxies in advanced morphological types belong to the advanced grouping (Groups 4~5). According to our calculation, this general tendency is understood as a variation of electron density inside the nuclei from lower to higher along the morphological types of galaxies.

As for the electron temperature, it varies in a range of $2 \sim 4 \times 10^4 °K$. But this range may be much extending to the high temperature side, since the galaxies show [OIII] line in appreciable strength are not included in the above consideration.

The total amount of ionized gas in the nuclear region of each galaxy can be deduced only when the absolute energy flux in emission lines is measured. Although we have no such measurement for normal galaxies up to the present, indirect information from some peculiar galaxies such as NGC 1068 [OSTERBROCK-PARKER (1965)], NGC 1275 [SEYFERT (1943)] (or cf. SATO, 1966) seems to suggest that the mean electron density averaged over the whole volume of the nucleus could not exceed $10^2 cm^{-3}$ even in its extremity. If it were so, the electron density obtained here would be generally quite high, and it inevitably would lead to the inhomogeneous structure of ionized gases in the nuclei of galaxies. At a glance, cloud structure of ionized gas seems to be hopeful, i. e., this is an idea that the ionized gas is concentrated to a small volume of the uncleus which is divided into innumerable cloudlets of high electron density. The kinetic energy is to be supplied from the cloud-cloud collisions. Each cloudlet is easily heated up to $10^5 °K$ by the collision with relative velocity of about 100 km/sec.

This picture, however, meets a serious difficulty for explaining the energy balance. That is, the cooling time of cloudlets is quite rapid, less than 10^2 years when the electron density exceeds $10^4 cm^{-3}$, Whereas the mean collision time of cloudlets is longer than at least 10^4 years so long as the mean size of cloudlets is taken to be larger than that of the order of planetary nebulae ($\sim 10^4$ A. U.). This discordance seems insuperable even if the appearance of emission lines could be attributed to some transient phenomena accompanied by explosive activity in the nuclei of galaxies. As for the actual physical processes, further investigation is quite desirable.

c) Comment on the collisional ionization degree.

In computing the ionization degree of the elements other than hydrogen, we have made use of the PARKER's (1964) formula, which is based on the ELWERT's (1952) formula by the hydrogen-like approximation. This may be compared with those of HOUSE (1964) and of OSTERBROCK-PARKER (1965). The ionization curves by these formulae generally coincide with each other for most of the elements in the temperature range of $1 \sim 10 \times 10^4 °K$. For some elements, say, oxygen, however, the ionization curves of OSTERBROCK-PARKER appreciably deviate from those of others. This deviation is mainly caused by the inclusion of the dielectronic recombination in the evaluation of OSTERBROCK-PARKER. Since the dielectronic recombination is an additional process of recombination the ionization degree is to be depressed. Fig. 5 shows the ionization curves for oxygen, the effect of dielectronic recombination being quite remarkable in the range of $T_e > 5 \times 10^4 °K$.

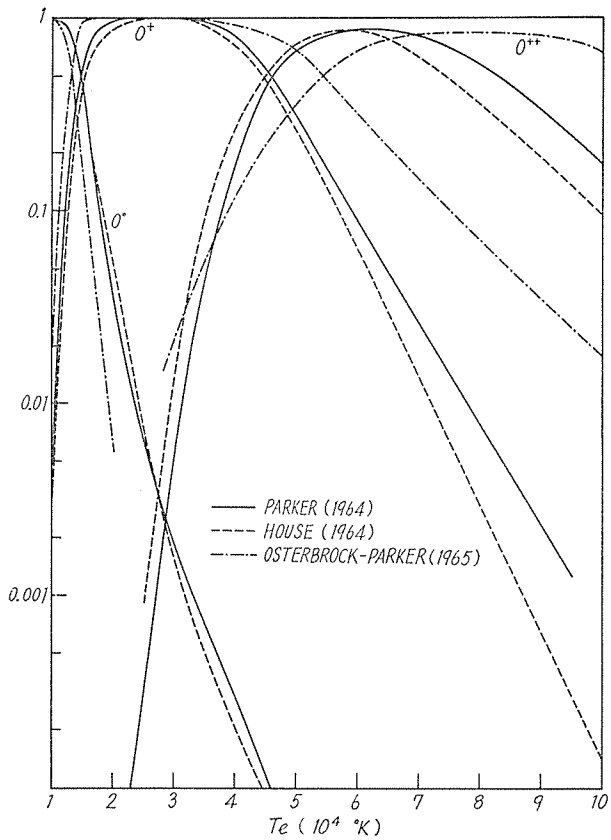

Fig. 5. Ionization degree of oxygen.
Of these three kinds of curves, we adopt PARKER's ones in the present paper.

In the present calculation, since this effect is not taken into account, the relative intensities [OIII]/[OII] is somewhat over-estimated in these temperature regions. In reality, the iso-intensity curve of [OIII]/[OII] would be shifted to the right-hand side in Fig. 4. Closer investigation is desirable in this point, particularly for galaxies showing [OIII] in appreciable strength. In the next place, we shall make some remarks on the discussion of B-G-P (BURBIDGE-GOULD-POTTASCH (1963)), who argued that the variation of relative intensities, say, of H_α/[NII] and [OII]/[NII], from the nuclear region to the outer part of galaxies could be explained by the variation of electron temperature of ionized gas. In reducing this conclusion, they have made use of the expression f for each ion, defined as

$$f(X^J)\equiv\frac{N(X^J)}{\sum_J N(X^J)}$$

where $N(X^J)$ denote the number density of the element X in the J-th stage of ionization, and put $f(X^J)/f(Y^K)=1$ for ions X^J and Y^K in some suitable temperature region. Particularly they assumed $f(N^+)/f(O^+)=1$ for $5\times10^{3\circ}K<T_e\lesssim2\times10^{4\circ}K$ and tried to explain the variation of relative intensity $I(N^+)/I(O^+)$. If, however, the ionization degree for N and O is evaluated by the present formula, their

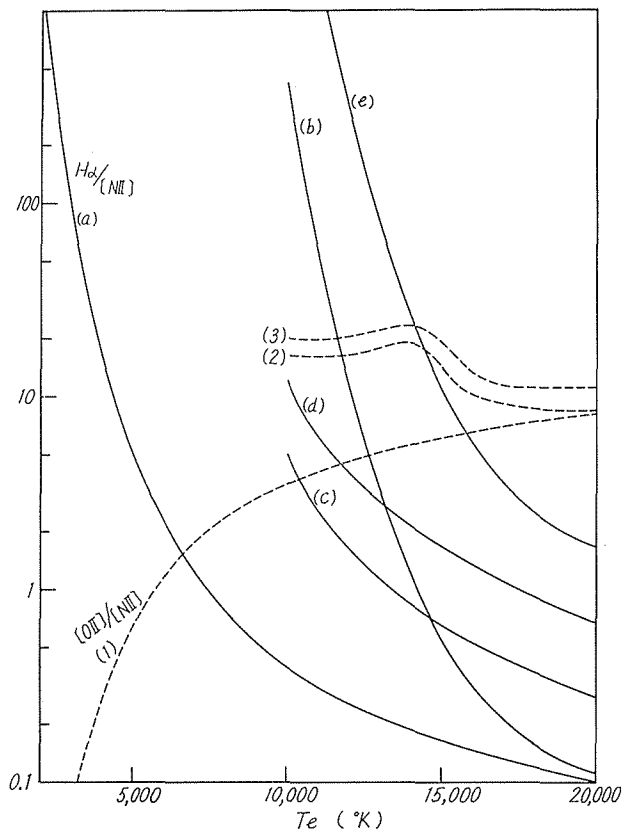

Fig. 6. H_α/[NII] and [OII]/[NII] intensity ratios.
(1), (a) : Original curve of B-G-P.
(2), (b) : Modified curve of B-G-P with respect to the values of f.
(3) : Curve computed in the present paper.
(c), (d), (e) : Our curves in Cases 1, 2a, and 2b, respectively.

conclusion should be altered. This circumstance is shown in Fig. 6, where the temperature of the relative intensities [OII]/[NII] and H_α/[NII] are given in some cases different in the treatment of f-values. From the inspection of Fig. 6, the following remarks may be given:

1) [OII]/[NII]……Curve 1 is the original B-G-P curve in which $f(N^+)/f(O^+)=1$ is assumed. Curve 2 is their modified curve by taking the temperature dependence of $f(N^+)/f(O^+)$ into account by the present ionization formula. Curve 3 is the one calculated here by us. It is to be noticed that the temperature dependence is much reduced when the variation of f is introduced.

2) H_α/[NII]……Curve a is B-G-P's original one, whereas curve b is their modified one for the variation of f-values. Curves c~e are ours in different cases for hydrogen, Cases 1, 2a, and 2b, respectively, both for $N_e=100$. Our curves, especially curve e of Case 2b, differ from ones of B-G-P remarkably. Here again we can see the important role of collisional excitation from the second energy level of hydrogen.

Moreover, it should be noted that these relative intensities largely depend

upon the variation of electron density of ionized gas when the electron density exceeds about $10^4 cm^{-3}$. This means that the situation in the variation of emission spectra is not so simple as suggested by B-G-P.

The authors wish to express their gratitude to Prof. T. SHIMIZU for constant encouragement and his reading the manuscript, and to Dr. M. KANNO who kindly send them the unpublished data on the cross-sections of collisional processes in hydrogen atoms.

Appendix. *Data on the Emission-line Spectra in Nuclei of Galaxies*

The data on the appearance of emission line spectra in nuclei of galaxies are compiled in Table A1 by making use of papers available for us at present. The galaxies are collected by the condition that the existence or absence of at least three lines of [OII]λ3727, [NII]λ6584 and H_α is specified in the nucleus of the galaxy. In Tables A1 and A2, the abbreviation for the designation of emission lines is made of as follows: *

OII = [OII]λ3727 (= $\lambda\lambda$3726+3728)
N = [NII]λ6584
α, β = H_α, H_β
OIII = [OIII]λ5007

Table 1 gives the descriptions of these emission lines. Each column gives the following:

column (1) : NGC number
(2) : Morphological type
(3) : Emission lines whose presence is affimative
(4) : Emission lines whose absence is affirmative
(5), (6), (7) : Relative line intensities of H_α/[NII], H_α/H_β and [OIII]/[OII], respectively.
(8) : Reference

The galaxies in Table A1 may be temporarily classified by the appearance of emission lines into several groups as follows:

Group 1. Only [OII] is detected.
2. [OII] and [NII] are detectable.
3. [OII], [NII] and H_α are all detectable.
4. [OII], H_α are detectable, but [NII] is much weaker than both of these.
5. [NII] and H_α are detectable.
6. [OIII] are stronger than [OII].
7. Relative intensities are unknown, but [OIII] is detected with definite strength.

Some of these groups may be divided according to the relative intensities into several subgroups such as shown in Table A2, which contains the galaxies belonging

* In the text, the intensity of forbidden line is given in the total strength of doublet i. e., [NII]$\lambda\lambda$6584+6548, [OIII]$\lambda\lambda$4959+5007, [OII]$\lambda\lambda$3726+3728. Attention should be paied when comparison is made between theoretical intensity in the text and the observed one in the Appendix. The relative intensities between two components of each doublets are as follows: [NII]λ6584/[NII]λ6548=2.8, [OIII]λ5007/[OIII]λ4959=2.7. The intensity of [OII] is always taken as the sum of λ3726 and λ3728.

Table A1.

NGC	Type	Emission Line		Relative Intensities			Reference
		Presence	Absence	$\frac{\alpha}{N}$,	$\frac{\alpha}{\beta}$,	$\frac{OIII}{OII}$	
128	SOp	OII, N	α	<1			BB'65
404	SO	OII, N, α		2			BB'65
613	SBb(Sb)	OII, α, N, β	OIII	$\gtrsim 1$		($\sim$0)	HMS'56, BB'62, '65
681	Sa	OII, N, α		1			BB'65
821	E6		OII, N, α				BB'65
925	Sc	OII, N, α		>3			BB'65
1052	E3	OII, N, α, OIII		1			BB'65
1068	Sbp	OIII, α, OII, N, β		1.8	12	17	Sey'43
1209	E6	OII, N	α	<1			BB'65
1275		OIII, α, OII, N		>1			Sey'43
1300	SBb	OII, α, N	OIII	$\sim$1	($\gg$1)	($\sim$0)	HMS'56, May'58 BB'62,'65
1316	SOp	N, OII	α	<1			BB'65
1415	Sa	OII, N, α		4			BB'65
1453	E1	N, OII	α	<1			BB'65
1530	SBc	α, N	OII	3			BB'65
2146	Sap(Sbp)	OII, α, N		2			HMS'56, BBP'59, BB'65
2655	SOp	OII, N	α	<1			BB'65
2685	SOp	OII, N	α	<1			BB'65
2749	E2	OII, N	α	<1			BB'65
2782	Sa	OII, N, α		3			BB'65
2814	E	OII	OIII, N, α			($\sim$0)	P'52
2820	E	OII	OIII, N, α			($\sim$0)	P'52
2855	SO	OII, N	α	<1			BB'65
2903	Sbc(Sc)	α, N, OII		$\sim$3			HMS'56, May'58, BB'62,'65
2911	SOp	OII, N	α	<1			BB'65
2974	E4	OII, N	α	<1			BB'65
3031	Sb	OII, α, N					HMS'56, Spr'62, B'62
3034	Ir	α, β, N, OIII, OII		3	steep		HMS'56, May'60, BB'62,'65
3065	SO	OII, N	α	<1			BB'65
3066	Sb	OII, N, α		3			BB'65
3166	Sa	OII, N	α	<1			BB'65
3185	Sa	OII, N, α		2			BB'65
3198	Sc	OII, N, α	OIII, β	$\sim$1	($\gg$1)	($\sim$0)	HMS'56, May'58,'60 BB'62, '65
3226	E1	OII, N	α	<1			BB'65
3395	Sc	OII, β, OIII, α, N		$\sim$4	$\sim$2	0.8	HMS'56, May'58, P'52
3396	Sc	OII, α, OIII, N		$\sim$1.6	$\sim$2	0.6	〃
3489	SOp	OII, N	α	<1			BB'65
3504	SBb(Sb)	α, N, OII, OIII		$\sim$3	$\gg$1	$<$1	BBP'60, BB'62, '65
3556	Ir	OII, α, N, β		$\sim$3			HMS'56, BBP'60, BB'62,'65
3593	SOp	OII, α, N		3			BB'65
3619	SO	OII	N, α	—			BB'65
3623	Sa	OII, N	α	<1			BBP'61b, BB'62, '65
3718	SOp	OII	N, α	—			BB'65
3769	SBc	OII, α, N		$\sim$2			P'52
3786	S	OIII, OII, N, α	(β)	1.7	steep	1.6	P'52
3898	Sa	OII	N, α				BB'65
3962	E1	OII, N	α	<1			BB'65
3998	SO	OII, N, α		1			BB'65
4038	Sc	OII, α, β, N	(OIII)	$\sim$2	$\sim$2	($\sim$0)	P'52
4039	Sc	α, β, OII, N	(OIII)	$\sim$4	$\sim$2	($\sim$0)	P'52
4105	E2	OII	N, α				BB'65
4106	SBO	OII	N, α				BB'65
4125	E6	OII, N	α	<1			BB'65
4151	Sa	OII, OIII, N, α		>1			HMS'56, Spr'62, Sey'43
4258	Sb	OIII, OII, N, α		0.3		>1	BB'62, '65
4278	E1	OII, α, N, β, OIII		1.2 0.7	1.3	0.25	Ost'62, P'52 BB'65

NGC	Type	Emission Line		Relative Intensities			Reference
		Presence	Absence	$\frac{\alpha}{N}$,	$\frac{\alpha}{\beta}$,	$\frac{OIII}{OII}$	
4314	SBa	OII, N, α		3			BB'65
4374	SO	OII, N	α	<1			BB'65
4438	SOp	OII, N, α		0.3			BB'65
4449	Ir	α, OIII, OII, β, N		>3	$\gg1$	>1	May'60, BB'62, '65
4485	Sc	OII	OIII, N, α, β			0	P'52
4486	E	OII, N					May'58, Spr'62
4490	Sc(Ir)	OII	OIII, N, α, β			0	P'52, May'60
4550	E7	OII	N, α				BB'65
4567	Sb(Sc)	α, N	OII, OIII, β	2			May'58, P'52, HMS'56
4568	Sb(Sc)	α, N	OII, OIII, β	4			〃
4631	Sc(Ir)	α, OIII, OII, N		>3	$\gg1$	>1	BB'62, '65
4636	EO	OII, N	α	<1			BB'65
4647	Sc	α, OII	OIII, N, β	($\gg1$)	($\gg1$)	(0)	HMS'56, May'58, P'52
4649	E2	OII	OIII, N, α, β			0	P'52, May'58, '60, HMS'56 Spr'62
4736	Sb	OII, N	OIII, α, β	<1		0	HMS'56, May'58, Spr'62 BB'62, '62a
5005	Sb	OII, N	α	0			HMS'56, May'60, BBP'61a BB'62, '65
5055	Sb	OII, N, α		(3)			HMS'56, May'60, Spr'62 BB'62
	Sc	OII	N, α				BB'65
5077	E3	OII, N	α	<1			BB'65
5194	Sc	OII, α, OIII, N		$\gg1$		0.6	P'52, Spr'62
		N, α		<1			BB'65
5195	Ir(Ep)	α, N	OII?	$\gg1$			P'52, Spr'62
	SO	OII, N	α	<1			BB'65
5253	Ir	α, β, OIII, OII, N		>3	($\gg1$)	($\gg1$)	B'62, BB'62, '65
5257	Sb	α, OII, N	OIII, β	4	$\gg1$	0	P'52
5258	Sb	α, OII, N	OIII, β	1	$\gg1$	0	P'52
5426	Sbc	OII, α, N	OIII, β	2	$\gg1$	0	P'52
5866	SO	OII, N	α	<1			BB'65
5929	EO	OII, α, N	OIII, β	3	$\gg1$	0	P'52
5930	E2	α' N, OII	OIII, β	1.6	$\gg1$	0	P'52
5953	E	α, N, OII	OIII, β	1.7	$\gg1$	0	P'52
5954	Sc	α, N, OII	OIII, β	3	$\gg1$	0	P'52
6503	Sc	N, α, OII	OIII	$\lesssim1$		0	HMS'56, BB'62, '65
6643	Sc	α, N, OII		$\gtrsim1$			HMS'56, BB'62, '65
7331	Sb	N, OII	OIII, α	<1		0	〃
7479	SBb	OII, N, α	(OIII)	<1		<1	HMS'56, May'58, BB'62
7640	SBc	OII, α, N		>1		<1	HMS'56, May'58, '60 BB'62, '65
7679	SO	OII, N, OIII, α, β		2			BB'65
7727	Sa	OII	N, α	—			BB'65
7743	SBa	OII	N, α	—			BB'65

Notes : Sey : SEYFERT
P : PAGE
HMS : HUMASON–MAYALL–SANDAGE
May : MAYALL
BBP : BURBIDGE–BURBIDGE–PRENDERGAST
Spr : SPINRAD
Ost : OSTERBROCK
B : BURBIDGE
BB : BURBIDGE–BURBIDGE
The number such as '43 mean the published year.

Table A2.

Groupe	Emission lines	Subgrouping	$r=\frac{\alpha}{N}$	E	SO	Sa	SBb, Sb	SBc, Sc, Ir
1	OII		—	2814 2820 4105 4649 4550	3619 3718 4106	3898 7727 7743		4485 4490
2	OII, N	OII>N	—	4486				
		OII<N	—				7331	
		OII, N	—	1209 1453 2749 2974 3226 3962 4125 4636 5077	128 1316 2655 2685 2855 2911 3065 3489 4374 5866	3166 3623	4736 5005	
3	OII, N, α	OII>N>α	<1					
		OII≲N≈α	~1				5258	
		OII≲N<α	>1	5930 5953			3504	2903 3034 5954
		OII≈α>N	>1	4278 5929			5257 5426	3395 3396 3769 4038 4039
		OII, N>α	<1		4438		7479	5194[a]
		OII, N≲α	≳1		404 3593 3998 5195[b]	681 1415 2782 3185 4314	613 1300 2146[e] 3066	925 3198 3556 6503 6643 7640
		OII, N, α	—				3031	
4	OII, α	OII, α	>1					5055[d]
		OII<α	>1					4647
5	N, α	N, α	—					
		N≲α	≳1				4567 4568	1530
		N>α	<1					
6	OIII>OII, N, α		—			4151[e]	1068[e] 1275[e] 3786[f] 4258	4449 4631 5253[g]
7	OIII, OII, N, α		—	1052	7679			

Notes:

a) [NII] and H_α, with the ratio $r=\alpha/N<1$, are detected by BB'65, while the relative intensity [OII] : H_α : [OIII] : [NII] = 5 : 3 : 3 : — was derived by P'52. In the latter we may have $r>1$, but we follw the new data of BB'65.

b) [OII], [NII] and no H_α are detected by BB'65 with the type SO, whereas H_α and [NII] are detected by P'52. Morphological type was classified by Ir or E_p by Spr.'62.

c) The type Sb_p due to BB'65 is used instead of Sa_p due to HMS'65.

d) H_α is detected by Spr.'62, though only [OII] and no [NII], H_α are found by BB'65.

e) Seyfert galaxy.

f) The morphological type is provisional since the designation by P'52 is only given as spiral.

g) Haro galaxy.

to each of these subgroups. The table is composed of as follows.

column (1) : Group number

(2) : Emission lines detectable in each group.

(3) : Relative intensities by which the subgroup is specified. Two emission lines are connected by equality, inequality or by comma according to their relative intensity, the comma being used when the relative intensity is uncertain.

(4) : Relative intensity between H_α and [NII].

(5)~(9) : NGC number of galaxy. Each column gives separate morphological type.

When some discordance is found in the appearance of emission lines among different references, we adopt the one favourable to existence. For the morphological type of galaxies we adopt the data of latest source of reference.

REFERENCES

ALLEN, C. W., 1955 *Astrophysical Quantities*, First edition, Univ. of London, London, Chap. 3.

BAADE, W., & N. U. MAYALL, 1951, *Problems of Cosmical Aerodynamics*, (Proceedings of the Symposium on the Motion of Gaseous Masses of Cosmical Dimensions held at Paris, Central Air Force Documents Office) Chap. 24, p. 165.

BAKER, J. G. & D. H. MENZEL, 1938, *Ap. J.*, 88, 52.

BURBIDGE, E. M., G. R. BURBIDGE, and K. H. PRENDERGAST, 1960, *ibid.*, **132**, 640.

—— , 1961a, *ibid.*, **133**, 814.

—— , 1961b, *ibid.*, **134**, 232.

BURBIDGE, E. M. & G. R. BURBIDGE, 1962a, *ibid.*, **135**, 366.

—— , 1962b, *ibid.*, **135**, 694.

—— , 1965, *ibid.*, **142**, 634.

BURBIDGE, E. M., 1962, *Interstellar Matters in Galaxies*, ed. L. WOLTJER, Benjamin Inc. New York, p. 123.

BURBIDGE, G. R., R. J. GOULD, & S. R. POTTASCH, 1963, *Ap. J.*, **138**, 945.

BURBIDGE, G. R., E. M. BURBIDGE, & A. R. SANDAGE, 1963, *Rev. Mod. Phys.*, **35**, 947.

CHAMBERLAIN, J. W., 1953, *Ap. J.* **117**, 387.

DE JAGER, C., M. KANNO, & L. H. NEVEN, 1960, *Ann. d' Ap.*, **23**, 843.

ELWERT, G., 1952, *Zs. f. Naturf.*, **7a**, 432.

GARSTANG, R. H., 1951, *M. N.*, **111**, 115.

—— , 1960, *M. N.*, **120**, 201.

GOLDBERG, L., E. A. MÜLLER, & L. H. ALLER, 1960, *Ap.* J., *Suppl.* **5**, 1.

HOUSE, L. L., 1964, *Ap. J., Suppl.* 8, 307.

HUMASON, M. L., 1947, *P. A. S. P.*, **59**, 180.

HUMASON, M. L., N. U. MAYALL, & A. R. SANDAGE, 1956, *A. J.*, **61**, 97.

JOHNSON, H. M., 1953, *Ap. J.*, **118**, 370.

MAYALL, N. U., 1939, *Lick Obs. Bul.*, **19**, 33.

—— , 1958, *IAU Symp.*, No. 5.

—— , 1960, *Ann. d' Ap.*, **23**, 344.

MINKOWSKY, W., 1955, *Gas Dynamics of Cosmic Clouds*, ed. H. C. van de HOLST and J. M. BURGERS, North-Holland Publ. Comp. Amsterdam, Chap. **18**, p. 106.

MINKOWSKY, R., & D. E. OSTERBROCOK, 1959, *Ap. J.* **129**, 583.

MIYAMOTO, 1956, *Zs. f. Ap.*, 38, 245.

OSTERBROCK, D. E., 1960, *Ap. J.*, **132**, 325.

—— , 1962, *Interstellar Matter in Galaxies*, ed. L. WOLTJER, W. A. Benjamin Inc., New York, p. 111.

OSTERBROCK, D. E. & A. R. PARKER., 1965, *Ap. J.*, **141**, 892.

PAGE, T., 1952, *ibid.*, **116**, 63.
PARKER, A. R., 1964, *ibid.*, **139**, 208.
SATO, F., 1966, *Publ. A. S. Japan*, in print.
SCHMIDT, M., 1965, *Ap. J.*, **141**, 1.
SEATON, M. J., 1955, *M. N.*, **114**, 154.
—— , 1958, *Rev. Mod. Phys.*, **30**, 978.
—— , 1959, *M. N.*, **119**, 81.
SEYFERT, C. K., 1943, *Ap. J.*, **97**, 28.
SPINRAD, H., 1962, *ibid.*, **135**, 715.
WOLTJER, L., 1959, *ibid.*, **130**, 38.